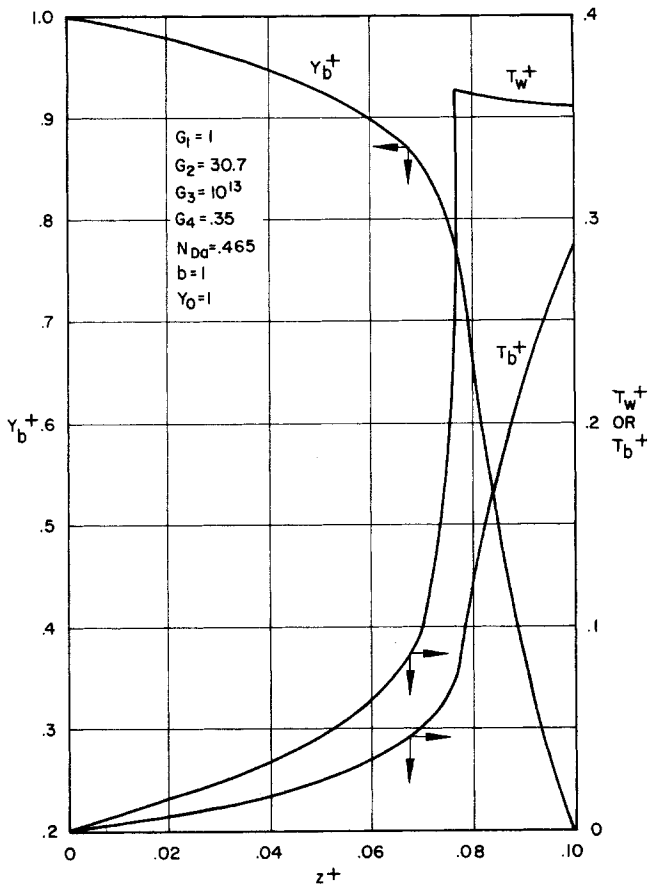

Fig. 19. Axial temperature and concentration profiles for an adiabatic exothermic reaction.

i = substance i
o = initial condition
p = point value
R_o = evaluated at wall
r = radial component
z = axial component

Superscripts

$+$ = dimensionless variable
$''$ = plug flow value
0 = entrance value

Operators

d = ordinary derivative
∂ = partial derivative
Δ = delta, change or increment
Σ_i = summation operator

LITERATURE CITED

1. Hougen, O. A., and K. M. Watson, "Chemical Process Principles," Vol. 3, Wiley, New York (1950).
2. Sandler, Samuel, and Yu Ho Chung. *Ind. Eng. Chem.*, **53**, 391-394 (1961).
3. Steacie, E. W. R., and I. E. Puddington, *Can. J. Res.*, **16B**, 176-193 (1938).
4. Cleland, F. A., and R. H. Wilhelm, *AIChE J.*, **2**, 489-497 (1956).
5. Trombetta, M. L., and John Happel, *ibid.*, **11**, 1041-1050 (1965).
6. Rothenberg, R. I., Ph.D. dissertation, Univ. Calif., Davis (1964).
7. Andersen, T. S., M.S. thesis, Univ. Pittsburgh, Pa. (1967).
8. Bird, R. B., W. E. Stewart, and E. W. Lightfoot, "Transport Phenomenon," Wiley, New York (1960).
9. Lapidus, Leon, "Digital Computation for Chemical Engineers" McGraw-Hill, New York (1962).

Manuscript received May 8, 1968; revision received December 16, 1968; paper accepted December 18, 1968.

Heterogeneous Reactions in the Photochlorination of Propane

BRUNO BOVAL and J. M. SMITH

University of Californ' Davis, California

An experimental study of the photochlorination of propane was undertaken to assess the significance of heterogeneous termination steps (wall reactions). Data were obtained in 2- and 10-mm. I.D. tubular flow reactors with varying oxygen concentrations. The results indicated that homogeneous terminations were dominant in the large reactor, and heterogeneous ones were dominant in the small unit. A kinetic scheme which explained the data was proposed. It included two parallel termination steps: a second-order homogeneous reaction between $C_3H_7\cdot$ and oxygen and a first-order heterogeneous reaction between $C_3H_7\cdot$ and the reactor wall.

Even though the data were taken in the laminar flow regime, the rate of reaction was a function of Reynolds number for the 10-mm. reactor. Kinetic factors may explain these results, but the reasons are not clear. More research in this area is needed.

Data taken in the 10-mm. reactor packed with quartz cylinders gave results similar to those for the 2-mm. reactor. This provided confirming evidence for the proposed scheme of parallel, heterogeneous and homogeneous termination steps.

There is compelling evidence (*12* to *14*) that photochlorinations occur by free radical, chain reactions in which termination steps may be heterogeneous as well as homogeneous. The significance of heterogeneous reactions is particularly important in scaling-up tubular-flow photoreactors because of the variation in surface-to-volume ratio

with diameter. Also, if wall steps are significant, the rate at a given axial position in the tube may depend upon radial transport rates of the reacting species, quantities that are difficult to evaluate for free radicals. Homogeneous termination processes are often strikingly influenced by small amounts of impurities in the reaction mixture.

Earlier work (*4*) on the gaseous photochlorination of propane in a 2-mm. I.D. reactor established kinetic constants but did not provide information on the nature of the chain terminating reactions. Investigation of wall deposits (*18*) has shown that if heterogeneous reactions are significant, such deposits have little effect on the rate.

This paper presents kinetic data and analysis designed to elucidate the nature of the chain-breaking reactions. Kinetics of the gaseous photochlorination of propane was studied in differential, tubular-flow reactors. Conditions were chosen so that the wall was clean, and data were obtained in 2-mm. and 10-mm. I.D. reactors, at different oxygen concentrations and turbulence levels. Oxygen is known (*9, 13*) to be a severe inhibitor for photochlorinations. Light intensity, as well as concentrations, affects the rate. Therefore, it is necessary to express the kinetics data in terms of rate constants in order to study the relative importance of termination steps. To accomplish this, independent light intensity measurements were made in situ.

APPARATUS

The chlorinations were carried out in a reactor-lamp system surrounded by an elliptical reflector. The arrangement of apparatus, materials, and operating procedure was similar to that described earlier (*4*). The irradiated length was 100 mm. for the 2-mm. reactor and 10 mm. for the 10-mm. I.D. reactor, shown in Figure 1. Four jackets (dimensions in Table 1), three for filter solutions to change the light intensity, and an evacuated one, surrounded the reactor. Air for cooling was circulated through a jacket surrounding a 150 mm. long, cylindrical lamp whose spectral characteristics are available (*16*). By changing the concentration of the filter solutions, the intensity of the radiation was changed, but the spectral distribution was held invariant and restricted to the range 3,000 to 3,500 Å. This was desirable in view of the possible variation of kinetic constants with wavelength. An important change from the earlier equipment was the provision to regenerate the silica gel drying tubes in place. This allowed better control of the oxygen in the feed by eliminating the introduction of air when the drying system was dismantled for regeneration.

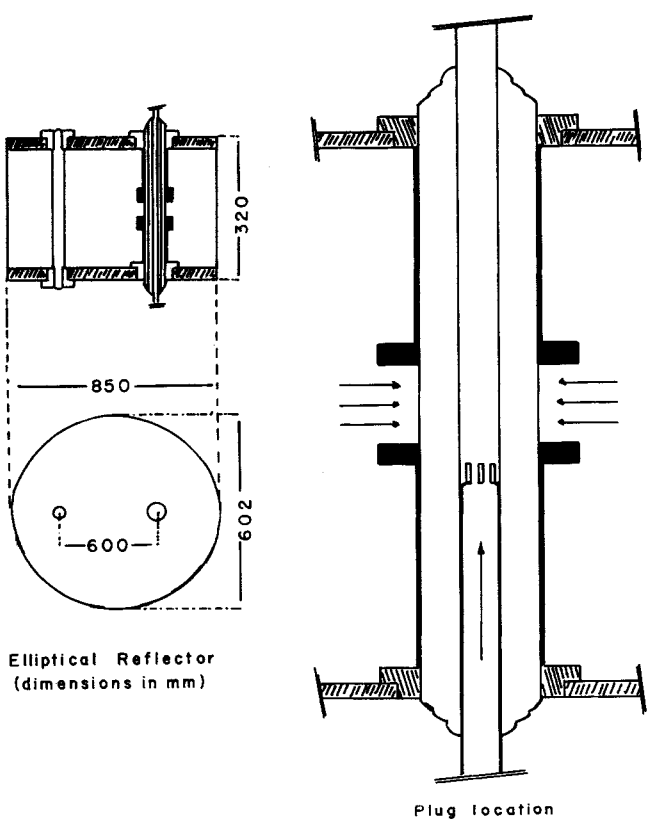

Fig. 1. Reactor system.

The reactor, jacket, and lamp walls were of fused, optically clear quartz which does not absorb light in the 3,000 to 3,500Å region. Cleaning the reactor walls with carbon tetrachloride, acetone, ethanol, and ether at periodic intervals (20 hr. for the 10-mm. reactor, 12 hr. for the 2-mm. unit) was sufficient to eliminate wall deposits.

The feed composition was varied from 0.3 to 1.1 mole % chlorine, with a molal propane-to-chlorine ratio of 4 (the remainder was nitrogen). Under these conditions differential reactor operation was achieved and only monochlorinated product (PrCl) obtained. Reactor temperature was 30 ± 1°C. and the pressure atmospheric. For the small reactor the specific rate of energy input σ was 0.160×10^2 Ein./(sec.)(mole), and for the large reactor data were obtained at two levels, $\sigma = 0.027$ or 0.106×10^2 Ein./(sec.)(mole). This quantity $\sigma = \sum_{\lambda} I_{w,\lambda}\alpha_{Cl_2,\lambda}$ is a measure of the light absorbed.

To change turbulence level in the large reactor, runs also were made with a porous plug containing four 0.059-in. holes. The plug was 2.0 cm. long with its downstream end located about 0.5 cm. before the feed entered the irradiated section of the reactor. Most of the runs were made without the plug and in the laminar flow region. The straight entrance section of the reactor had an L/D ratio of 33 for the large unit and 140 for the 2-mm. I.D. reactor.

The effect of oxygen was studied by using two kinds of nitrogen. The purer grade contained less than 30 p.p.m. of oxygen, and variations between individual cylinders was small. From the less pure grade cylinders were chosen that contained less than 100 p.p.m., but the amount varied from cylinder to cylinder.

The amount of reaction was established by analyzing the product gases for hydrochloric acid and unreacted chlorine (see reference *4*). Also, chlorine concentrations were measured in the effluent from a completely darkened reactor of the same size. This established the extent of the dark reaction, which was found to be negligible. This procedure also permitted making a total chlorine balance. The error in the mass balance was less than 2.5% for all the runs.

LIGHT INTENSITY MEASUREMENTS

Light intensities at the inside wall of the reactors were measured in situ by using photosensitized (with uranyl ions) decomposition of oxalic acid as actinometer. The procedure and precautions were the same as previously described (*4*). The decomposition is zero order so that the conversion of oxalic acid x_{ox} should be directly proportional to the average residence time V_R/Q. Figure 2

Table 1. Reactor Dimensions

	Small reactor	Large reactor
Diameter, mm.	2.0	10.0
Width of first jacket, mm.	10.5	6.5
Width of second jacket, mm.	2.5	2.5
Width of third jacket, mm.	5.5	5.5
Width of fourth jacket, mm.	7.5	7.5
Total diameter of assembly, mm.	69.0	69.0
Total length, mm.	750.0	750.0
Irradiated length, mm.	100.0	10.0

* First jacket is closest to the reactor.

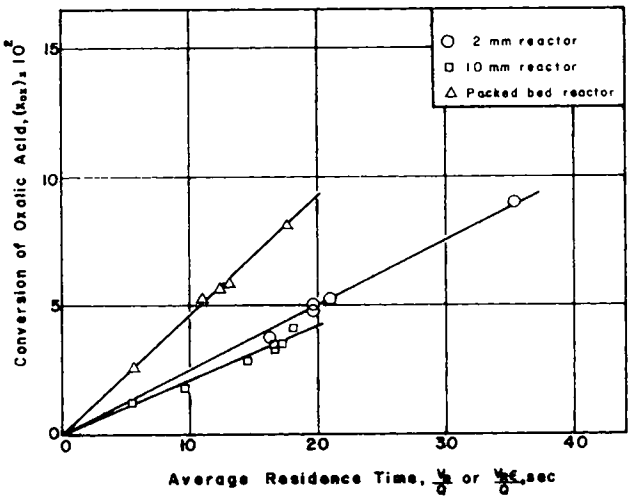

Fig. 2. Actinometer data.

shows that the data follow this requirement. From the measured conversion, the concentration of oxalic acid concentration in the feed, and V_R/Q the rate of the actinometer reaction was calculated according to

$$r_{ox} = \frac{(C_{ox})_o\, x_{ox}}{V_R/Q} \tag{1}$$

From knowledge of the rate and the quantum yield, the light intensity can be evaluated. The calculation is complicated by the filter solutions in the jackets around the reactor and the variation of intensity across the reactor diameter. The effect of the filter solutions was accounted for by measuring their transmittances, as a function of wavelength, in a spectrophotometer. These measurements gave an attenuation coefficient $(\mu_\lambda)_i$ for each solution i. Then the fractional transmission of the light through the three jackets around the reactor is given by

$$\theta_\lambda = \exp\left[- \sum_i (\mu_\lambda)_i\, \delta_i \right] \tag{2}$$

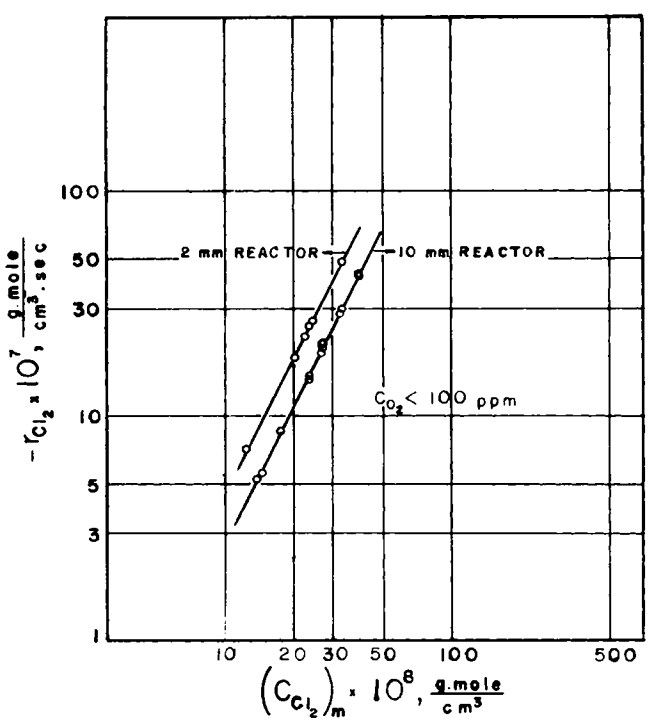

Fig. 3. Second-order dependency of rate on chlorine concentration.

The intensity of interest is that at the inside wall of the reactor for chlorination studies, that is, $I_{w,\lambda}$. This is calculated by a two-step process. The key quantity is $I_{b,\lambda}$, which is the intensity at the wall of the reactor if there were no filter solutions. It is calculated from the actinometer data from the following equation (see reference 4):

$$I_{b,\lambda} = \frac{\frac{R}{2} r_{ox}}{\sum_\lambda (\Phi_\lambda)_{ox} \frac{F_\lambda}{F_t} \theta_\lambda \left[1 - e^{-2R(\mu_\lambda)_{ox}} \right]} \tag{3}$$

where $(\mu_\lambda)_{ox}$ and $(\Phi_\lambda)_{ox}$ are the attenuation coefficient and quantum yield of the actinometer solution. These values are available (4) and are tabulated along with the output F_λ/F_t of the lamp in Table 2.* The second step is to calculate $I_{w,\lambda}$ from the fractional transmission T_λ for the filter solutions used in the jackets for the chlorination studies:

$$I_{w,\lambda} = I_{b,\lambda} \left(\frac{F_\lambda}{F_t} \right) T_\lambda \tag{4}$$

The filter solutions for the 2-mm. reactor were the same in actinometer and chlorination runs, so $\theta = T$ in this case. For the 10-mm. reactor, distilled water ($\theta_\lambda = 1.0$) was used in the actinometer measurements, and two different sets of filter solutions were used for the chlorination studies. The transmission coefficients, θ_λ or T_λ, are given in Table 3.*

Chemical filters are aqueous solutions of inorganic salts. With the aid of published information (3, *11* to *13*), the set of filter solutions I and II were prepared empirically to provide high and low transmittances of approximately the same wave length distribution.

In Table 4* are given the values of $I_{b,\lambda}$ and $I_{w,\lambda}$ calculated as described from Equations (3) and (4). Also the totals summed over all wavelengths are included. Equation (3) is based upon radially incident light striking the reactor. Owing to difficulties in centering the reactor and lamp at the focuses of the elliptical reflector, imperfections in the reflector itself, and the finite diameter of the lamp and reactor, the radially incident assumption is uncertain. Recently (*10*), this model was compared with the other extreme, completely diffuse light. The comparison was made between rate constants for gaseous decomposition of acetone, a system having similar absorptivities to those for chlorine. The results indicated that the rate constants calculated by the two models differed by less than 8%. Hence the uncertainty about the light pattern is not critical. This is particularly true in this study, since the results are based upon comparing rate constants for different operating conditions; absolute values are not significant. However, the $I_{b,t}$ values in the last two columns of Table 4* suggest that the actual light pattern more closely approaches the diffuse model than the radially incident model. Since the small reactor is one-fifth the diameter of the large one, the radial model would predict that $I_{b,t}$ for the 2-mm. reactor would be five times that of the 10-mm. reactor. Actually, the ratio of $I_{b,t}$ is 1.6. If the pattern were diffuse, $I_{b,t}$ would be the same for the two reactors.

RESULTS

Since the chlorinations were carried out under differen-

* Table 2 to 5 have been deposited as document 00927 with the ASIS National Auxiliary Publications Service, c/o CCM Information Sciences, Inc., 22 W. 34th St., New York 10001 and may be obtained for $2.00 for microfiche or $5.00 for photocopies.

Table 6. Effect of Light Intensity on Rate (10-mm. Reactor)

Run No.	N_{Re}	Filter solutions	$k_0 \times 10^{-8}$ cc./(g. mole)(sec.)	$\sigma \times 10^2$ Ein./(g. mole) (sec.)
49	460	I	0.489	0.106
50	460	I	0.507	0.106
65	467	II	0.098	0.027
66	467	II	0.106	0.027

$C_{O_2} < 30$ p.p.m.

tial reactor conditions, the rate could be calculated from the expression

$$-r_{Cl_2} = \frac{Q}{V_R}\left[(C_{Cl_2})_o - (C_{Cl_2})_L\right] \quad (5)$$

Previous work (*4, 5, 18*) had shown that the overall photochlorination was second order with respect to chlorine and zero order in propane at the concentrations employed. Preliminary data were taken over a range of chlorine and propane concentrations to test these conclusions in the present work. Figure 3 shows that straight lines are established, when plotting $-r_{Cl_2}$ vs. C_{Cl_2}, with a slope of 2. These data are for the impure nitrogen ($C_{O_2} < 100$ p.p.m.) and both reactors, but all the runs for each reactor were made with the same oxygen concentration (that is, same cylinder of nitrogen).

If the second-order rate constant k_o is defined by the expression

$$-r_{Cl_2} = k_o (C_{Cl_2})^2 \quad (6)$$

it may be calculated from the equation

$$k_o = \frac{Q}{V_R (C_{Cl_2})_o} \frac{x_{Cl_2}}{1 - x_{Cl_2}} \quad (7)$$

This rate constant is a function of the light intensity, the specific energy input σ, and the absorptivity of chlorine α_{Cl_2}. It has been shown (*4*) that the kinetic constant K, which is independent of these variables, can be calculated from k_o as follows:

$$K = \frac{k_o}{4\sum_{\lambda} I_{w,\lambda}\, \alpha_{Cl_2,\lambda}} = \frac{k_o}{4\sigma} \quad (8)$$

In Table 4,* $I_{w,\lambda}$ is given for each reactor and each series of filter solutions. From this information and the published data (*19*) for chlorine absorptivities, σ can be calculated. Complete results are given in Table 5,* but the pertinent values are $\sigma = 1598. \times 10^6$ (v.) (Ein.)/(g. mole) (sec.) for the 2-mm. reactor; $\sigma = 1064. \times 10^6$ and 267.8×10^6 (Ein.)/(g. mole) (sec.) for filter solutions I and II, respectively, in the 10-mm. reactor.

By using the observed data and σ, k_o and K were calculated from Equations (7) and (8). The significance of the termination steps was studied by comparing these kinetic constants for different operating conditions. The pertinent results are analyzed in the subsections that follow. It is of interest to note the effect of light intensity upon the rate, as established by the measurements in the large reactor with series of filter solutions I and II. The results are shown in Table 6. While there are but two intensity levels, the results indicate a linear relationship, in agreement with the much more extensive data published earlier (*4, 18*). Hence the results obtained in the present study show the same overall kinetics as observed in the earlier work.

Wall Stabilization

In the 10-mm. reactor, which was prepared from new quartz tubing, no stabilization period with varying rates was observed. Initial runs gave rate constants essentially the same as those at later times. This is indicated in Figure 4, where the rates for the same nitrogen cylinder are constant. Light intensity and Reynolds number were the same for all runs, but oxygen concentration varied from cylinder to cylinder when the less pure grade of nitrogen was used.

In marked contrast, k_o varied with time in the 2-mm. reactor, increasing for the first 160 hr. before attaining a stable value. These results are shown with a chronological time scale in Figures 5*a* and 5*b*. The oxygen content of the nitrogen did not affect the rate, as seen in Figure 5*b*, where the nitrogen cylinder was changed after the second series of actinometer runs. This reactor was not new but had been used previously for chlorination studies and subsequently cleaned with chromic acid solution, a strong oxidizing agent. It is clear that meaningful comparisons of reactors of different diameters should be made on new reactors. However the data of Cassano and Smith (*4*) in a new 2-mm. reactor also indicated a wall stabilization period, but only about 30 hr. in length.

Oxygen Effect

Figure 4 shows that different but reproducible values of k_o were obtained for each nitrogen cylinder in the 10-mm. reactor. Chromatographic analysis of the gas from this source indicated different oxygen contents for each cylinder, but in each case C_{O_2} was less than 100 p.p.m. Additional runs using nitrogen containing more than 100 p.p.m. of oxygen resulted in complete inhibition of the chlorination reaction. These results suggest that homogeneous termination steps involving oxygen affected the rate.

Reactor Diameter

In view of the effects of oxygen concentration and wall condition on the rate, comparison of data for different reactor diameters should be made for low and constant oxygen concentration and for equivalent wall conditions. The original data of Cassano and Smith (*4*) were obtained using a new 2-mm. reactor made from the same quartz as employed to construct the 10-mm. reactor used in the current study. Hence data were measured by using the 10-mm.

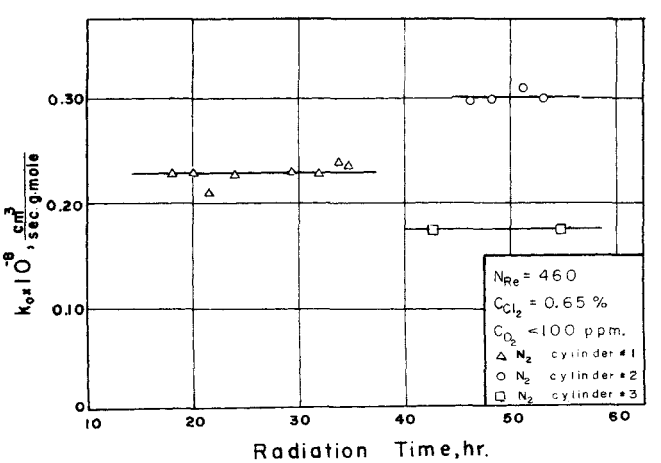

Fig. 4. Effect of oxygen concentration in 10-mm. reactor.

* See footnote on p. 555.

reactor and the same high purity nitrogen ($C_{O_2} < 30$ p.p.m.) as used in the earlier work. Comparison of these data should show the effect of surface-to-volume ratio. For this comparison rate constants K must be used, since σ varies with reactor diameter. The results are given in Figure 6. Two items are important. First, the rate constant is higher for the larger reactor, suggesting that heterogeneous termination reactions are important at least in the 2-mm. reactor. Second, the rate in the 10-mm. reactor is a function of Reynolds number, even though the flow was laminar at all flow rates.

Effect of Flow Rate

The effect of flow rate observed in Figure 6 cannot be due to failure to achieve a stationary state for the concentration of free radicals. It is important to check this possibility because Equations (6) to (8) for evaluating K are based upon the stationary state hypothesis. That this assumption is not responsible for the flow rate effect is evident from Figure 7. If stationary state were not attained, the rate constant would increase with residence time, ultimately reaching a constant value. Actually, the opposite effect is observed. To see if oxygen concentration could explain the effect, runs were also made with the lower purity nitrogen. The middle curve shows these data and indicates the same trend as found for the higher purity nitrogen (upper curve). It was concluded that the effect of flow rate is due to kinetic or radial diffusion resistance. For the latter to influence the rate, heterogeneous termination of free radicals would have to be important in the 10-mm. reactor. If this were true, in laminar flow the diffusion time for free radicals to reach the wall would decrease as the average residence time decreased. This would mean that the rate constant would increase with decreasing residence in agreement with the data in Figure 7.

To investigate radial diffusion, data were obtained with a porous plug installed just upstream from the reactor entrance. Introduction of turbulence in this way reduced the rate constant about 10% for the same oxygen concentration, as shown by the lower curve in Figure 7. This indicates that if heterogeneous termination steps are important in the 10-mm. reactor, the rate is not significantly affected by radial diffusion resistance. Thus radial diffusion could not explain the observed flow rate effect.

Discussion and Conclusions

The data show four results that are pertinent to the nature of the termination reactions. First, wall stabilization phenomena are important in the 2-mm. reactor but not in the 10-mm. reactor. Second, oxygen concentration affected the rate in the 10-mm. reactor but not in the 2-mm. reactor. Third, the rate constant was less in the small reactor at the same conditions, and, fourth, flow rate influenced the results in the large reactor.

The first three results suggest that heterogeneous termination reactions at the reactor wall controlled the overall chlorination rate in the 2-mm. reactor, while homogeneous steps were predominant in the 10-mm. reactor. In the earlier work it was pointed out that either homogeneous or heterogeneous termination steps, as long as they were first order, would lead to rate equations first order in light intensity and second order in chlorine concentration, that is, Equations (6) and (8). Hence, data at constant oxygen concentration in a single reactor did not provide enough information to distinguish between heterogeneous and homogeneous reactions. However, the information reported here allows more detailed study of the termination steps and indicates, in particular, that the homogeneous termination involves oxygen. The first three results can be explained by considering such a homogeneous step in parallel with a wall termination reaction.

We note first that all previous data (*4, 5, 18*) are explainable by assuming that termination of propyl radicals controls the process and that the activation and propagation steps are

$$Cl_2 + h\nu \xrightarrow{k_1} 2Cl \cdot \qquad (9)$$

$$Cl \cdot + PrH \xrightarrow{k_2} HCl + Pr \cdot \qquad (10)$$

$$Pr \cdot + Cl_2 \xrightarrow{k_3} PrCl + Cl \cdot \qquad (11)$$

On the basis of mechanism studies in the literature (*1, 2, 6* to *9, 15, 17*), likely termination steps for propyl radicals are

$$Pr \cdot + O_2 \xrightarrow{k_4} PrO_2 \cdot \quad \text{(homogeneous)} \qquad (12)$$

$$(\text{followed by } 2\,PrO_2 \cdot \xrightarrow{k_5} O_2 + \text{stable products})$$

$$Pr \cdot + \text{wall} \xrightarrow{k_{w2}} \text{end} \quad \text{(heterogeneous)} \qquad (13)$$

We will base the analysis on the assumptions that reactions (9) to (11) and termination steps (12) and (13) are sufficient to establish the overall rate. By using the stationary state hypothesis

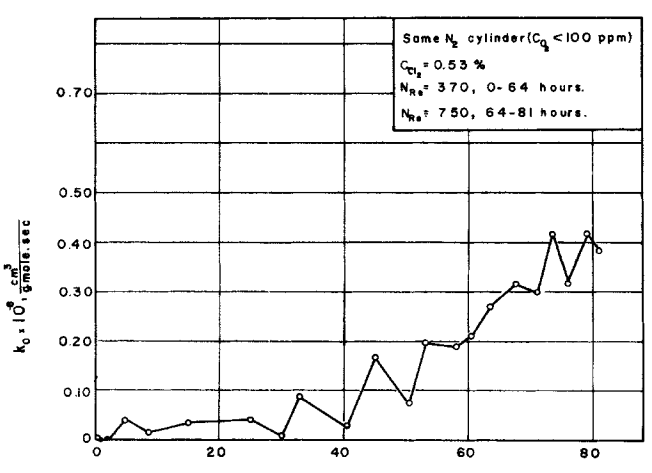

Fig. 5a. Wall stabilization in small reactor.

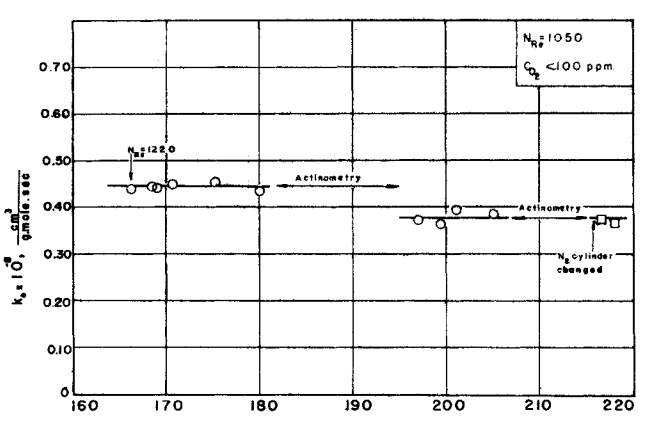

Fig. 5b. Wall stabilization in small reactor.

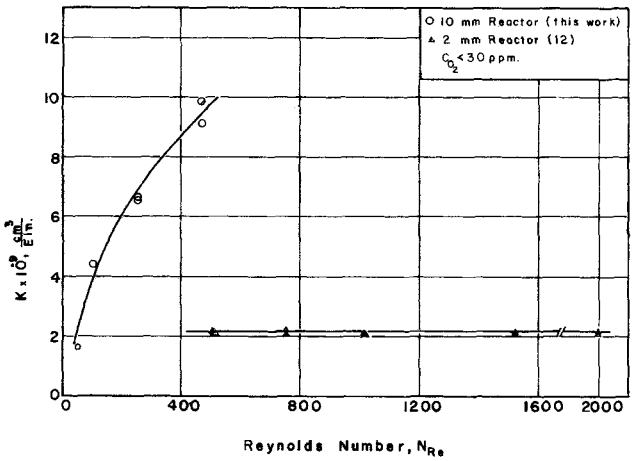

Fig. 6. Effect of reactor diameter.

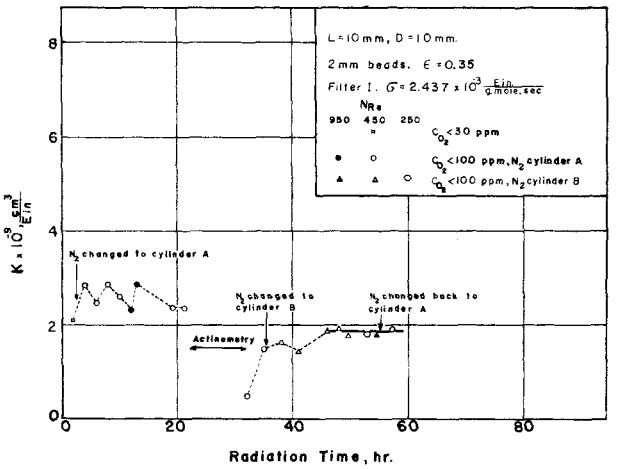

Fig. 8. Packed bed data.

$$\frac{dC_{Pr\cdot}}{dt} = k_2\,(C_{Cl\cdot})\,(C_{PrH}) - k_3\,(C_{Pr\cdot})\,(C_{Cl_2}) - k_4\,(C_{Pr\cdot})\,(C_{O_2}) - \frac{2}{R}k_{w2}\,(C_{Pr\cdot}) = 0 \quad (14)$$

$$\frac{dC_{Cl\cdot}}{dt} = 2\,k_1\,(\alpha_{Cl_2,\lambda})\,(C_{Cl_2})\,I_\lambda - k_2\,(C_{Cl\cdot})\,(C_{PrH}) + k_3\,(C_{Pr\cdot})\,(C_{Cl_2}) = 0 \quad (15)$$

where the rate of the termination step at the wall, $k_{w2}\,(C_{Pr\cdot})$, is per unit wall area and must be multiplied by $2/R$ to convert it to a rate per unit volume. By solving these two equations for $C_{Pr\cdot}$, the rate of disappearance of chlorine, according to Equation (11), is

$$-r_{Cl_2,\lambda} = r_{PrCl,\lambda} = k_3\,(C_{Pr\cdot})\,(C_{Cl_2}) = \frac{2k_1k_3\,(\alpha_{Cl_2,\lambda})\,I_\lambda\,(C_{Cl_2})^2}{\frac{2}{R}k_{w2} + k_4\,(C_{O_2})} \quad (16)$$

This expression gives the rate at a given wavelength λ and applies to a point in the reactor where the intensity is I_λ. Summing over the whole wavelength range and integrating across the reactor radius, for a differential reactor (constant concentrations), we get

$$-r_{Cl_2} = \frac{4\,k_1k_3}{\frac{2}{R}k_{w2} + k_4\,(C_{O_2})}\,\sigma(C_{Cl_2})^2 \quad (17)$$

The procedure of summation and integration is described in detail in (4). Now, a comparison of Equation (17)

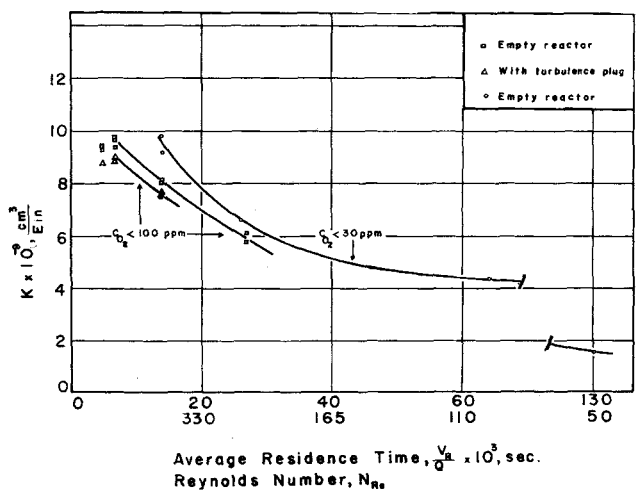

Fig. 7. Effect of flow rate in 10-mm. reactor.

with Equations (6) and (8) provides a more detailed description for K; that is

$$K = \frac{k_1k_3}{\frac{2}{R}k_{w2} + k_4\,(C_{O_2})} \quad (18)$$

This result shows that, in general, the rate constant will depend upon the oxygen concentration, the tube radius R, and the condition (activity for termination reaction) of the wall through k_{w2}. In the 2-mm. reactor there was a strong dependency of K (or k_o) on wall stabilization (Figure 6) and little dependency upon C_{O_2} (Figure 5*b*). This suggests that R was small enough to make the first term in the denominator of Equation (18) predominant. In contrast, in the 10-mm. reactor C_{O_2} had an effect on the rate (Figure 4), and no wall stabilization period was noted, suggesting that the $k_4\,(C_{O_2})$ term in Equation (18) was predominant. It appears that heterogeneous termination controlled the rate in the 2-mm. reactor, and homogeneous termination was controlling in the 10-mm. reactor.

The influence of flow rate (fourth result) is more complex. An effect was observed only in the 10-mm. reactor, where wall terminations do not seem to be dominant. Hence, it is difficult to explain the decrease in K with residence time (Figure 7) by a radial diffusion resistance. This is substantiated by the small decrease in K observed when a turbulence plug was inserted before the reactor. Perhaps there is an explanation associated with the kinetics scheme. The homogeneous termination of propyl radicals is described as a two-step reaction in series in Equation (12). If the concentration of PrO_2 radicals does not achieve steady state, the variation in C_{O_2} with residence time could explain the data. Estimates of k_4 and k_5 can be made from the literature (2, 8) and give $k_4 = 1 \times 10^{12}$ cc./(g. mole)(sec.) and a lower value for k_5, 10^9 to 10^{11} cc./(g. mole)(sec.). If stationary state is not achieved, at low residence times the oxygen would not be released by the decomposition of $PrO_2\cdot$ as fast as it was formed by Equation (12). Hence, the average C_{O_2} would be less for short residence times than for long times. Since homogeneous termination is believed to be controlling the rate, this would explain the decrease in K with increasing residence time observed in Figure 7. The trouble with this theory is the postulate that a stationary state is not reached with respect to $PrO_2\cdot$ but does exist for $Pr\cdot$ and $Cl\cdot$.

It should be noted that the data in Figure 7 are entirely within the streamline flow region so that the observed effect cannot be associated with a change from streamline to turbulent flow. It seems clear that more study is needed to elucidate the effect of flow rate on photochemical reac-

tions involving heterogeneous and homogeneous termination steps.

As a test of the conclusions, chlorination and actinometer (see Figure 2) runs were made with the 10-mm. reactor packed with optically clear, fused quartz cylinders, 2 mm. in diameter and in length. The 5 cm. long bed was held in position with perforated Teflon plugs; the irradiated bed length was 10 mm. and the void fraction ϵ estimated to be 0.35. With this packed bed reactor the surface-to-void volume ratio was 67, in comparison with 20 and 4 for the empty 2- and 10-mm. reactors. The rate constants for the chlorination runs and the chronological sequence of chlorination and actinometer measurements are shown in Figure 8. Several aspects of the results are significant. First, the increase in K with time initially, and after actinometry, suggests some surface stabilization period. Further evidence of surface effect is the difference in stabilized values of K before and after actinometry (during actinometer runs the surface is covered with aqueous solution of uranyl sulfate and oxalic acid). It is also noted that changing Reynolds number (based upon empty tube) from 250 to 950 had no effect on K. In addition, changing oxygen content by switching nitrogen cylinders did not appear to affect the results appreciably. Finally, the absolute value of K is about the same as that observed for the empty 2-mm. reactor (Figure 6). Quantitative comparison of rate constants for packed and empty reactors is hazardous because of the possible effects of reflections and distortion by the quartz particles. However, it is significant that K is of the same general magnitude for the packed and 2-mm. empty reactors. All aspects of the packed bed data suggest that heterogeneous termination steps were controlling the chlorination rate, as was found for the empty 2-mm. reactor. In view of the surface-to-volume ratio, this is what would be expected from the conclusions drawn from the empty reactor measurements and tends to confirm the form of Equation (18). Note that the coefficient of k_{w2} in that expression is the surface-to-volume ratio.

ACKNOWLEDGMENT

The financial assistance of the Water Pollution Control Board Administration through grant WP-00952 for partial financial support is gratefully acknowledged.

NOTATION

C = concentration, g. mole/cc.
F_λ = flux of the light source (lamp) at wavelength λ, Ein./sec.
F_t = total flux of lamp, Ein./sec.
I_λ = light intensity at wavelength λ, Ein./(sq.cm.)(sec.)
$I_{b,\lambda}$ = light intensity of wavelength λ at wall of reactor when no filter solutions are used in surrounding jackets; $I_{b,t}$ = total intensity over the wavelength range, Ein./(sq.cm.)(sec.)
$I_{w,\lambda}$ = light intensity of wavelength λ with filter solutions; $I_{w,t}$ = total intensity over the wavelength range, Ein./(sq.cm.)(sec.)
K = overall kinetic constant for chlorination, cc./Ein.
$k_{1,2,\cdots}$ = rate constants for specific, homogeneous reactions with appropriate units
k_{w2} = rate constant for wall termination reaction, Equation (13), (cc. of gas vol.)/(sec.)(sq.cm. of wall area)
k_o = overall, second-order rate constant, cc./(g. mole)(sec.)
L = illuminated length of reactor, cm.
Q = volumetric flow rate (30°C., 1 atm.), cc./sec.
r_{ox} = rate of actinometer reaction (rate of decomposition of oxalic acid), g. moles/(cc.)(sec.)
r_{Cl_2} = rate of formation of chlorine, g. moles/(cc.)(sec.)
R = radius of reactor tube, cm.
T_λ = fraction of incident light of wavelength λ transmitted through filter solutions used for chlorination studies
V_R = reactor volume, cc.
x = conversion; x_{ox} = conversion of oxalic acid in actinometer reaction; x_{Cl_2} = conversion of chlorine in photochlorination reaction

Greek Letters

α_{Cl_2} = molar absorptivity of chlorine, sq.cm./g. mole
δ_i = thickness of filter jacket i
μ_λ = attenuation coefficient for wavelength λ in actinometer system, cm.$^{-1}$
σ = specific rate of energy input = $\sum_\lambda I_{w,\lambda}\,\alpha_{Cl_2,\lambda}$, Ein./(g. mole)(sec.)
θ_λ = fraction of incident light of wavelength λ transmitted through filter solutions used for actinometer studies
Φ_λ = quantum yield at wavelength λ for actinometer system, g. moles/Ein.

Subscripts

L = condition at exit of reactor of length L
m = mean value
o = condition at reactor entrance

LITERATURE CITED

1. Bodenstein, M., and P. W. Schenk, *Z. Physik. Chem.*, **B20**, 420 (1933).
2. Burnett, G. M., and H. W. Melville, *Chem. Rev.*, **54**, 225 (1954).
3. Calvert, J. G., and J. N. Pitts, Jr., "Photochemistry," Wiley, New York (1966).
4. Cassano, A. E., and J. M. Smith, *AIChE J.*, **12**, 1124 (1966).
5. *Ibid.*, **13**, 915 (1967).
6. Fok, N. V., and Nalbandyen, "Problems of Chemical Kinetics, Catalysis and Reactivity," p. 219, Acad. Sci. USSR, Moscow, Russia (1955).
7. Göhring, R., *Z. Elektrochemie*, **27**, 511 (1921).
8. Goldfinger, P., G. Huybrechts, G. Martens, L. Meyers, and V. Olbregts, *Trans. Faraday Soc.*, **61**, 1933 (1965).
9. Jones, L. T., and J. R. Bates, *J. Am. Chem. Soc.*, **56**, 2282 (1934).
10. Matsuura, T., A. E. Cassano, and J. M. Smith, *Ind. Eng. Chem.*, to be published.
11. Noyes, W. A., Jr., ed. "Advances in Photochemistry," Vol. 1 (1963) and Vol. 2 (1964), Interscience, New York.
12. ———, and Boekelheide, in "Techniques of Organic Chemistry," Vol. 2, Arnold Weissberger, ed., Interscience, New York (1948).
13. Noyes, W. A., Jr., and P. A. Leighton, "Photochemistry of Gases," Reinhold, New York (1941).
14. Rollefson, G. K., and M. Burton, "Photochemistry and Mechanism of Chemical Reactions," Prentice-Hall, Englewood Cliffs, N. J. (1939).
15. Sleppy, W. C., and J. G. Calvert, *J. Am. Chem. Soc.*, **81**, 769 (1959).
16. *Technical Bulletin No. L-S-104*, Lamp Division, General Electric Company (1959).
17. Trifonov, A., *Z. Physik. Chem. (Leipzig)*, **33**, 195 (1929).
18. Ziolkowski, Dariusz, A. E. Cassano, and J. M. Smith, *AIChE J.*, **13**, 1025 (1967).
19. Gibson, G. E., and N. S. Bayliss, *Phys. Rev.*, **44**, 188 (1933).

Manuscript received October 1, 1968; revision received November 22, 1968; paper accepted December 11, 1968.